

Radiation effects on MHD free convective boundary layer flow of nanofluids over a nonlinear stretching sheet

T. Poornima and N. Bhaskar Reddy

Department of Mathematics, Sri Venkateswara University, Tirupati

ABSTRACT

The present study focuses on the numerical solution of a steady free convective boundary-layer flow of a radiating nanofluid along a non-linear stretching sheet in the presence of transverse magnetic field. The model used for the nanofluid incorporates the effects of Brownian motion and thermophoresis. The governing boundary-layer equations of the problem are formulated and transformed into a non-similar form. The resultant equations are then solved numerically using Runge-Kutta fourth order method along with shooting technique. In the absence of radiation parameter, magnetic parameter and for $m = 1$ (the non-linear stretching parameter), our results showed a good agreement with those of Anwar et al.[36] and also with that of Khan and Pop [34], for further reduced case. The physics of the problem is well explored for the embedded material parameters through graphs and tables. Further there is a scope of researching the reactions taking place in the mixture and the heat source /sink.

Keywords: Brownian motion, MHD, Nanofluid, Natural convection, Thermal radiation, Thermophoresis

INTRODUCTION

Nanofluids attract a great deal of interest with their enormous potential to provide enhanced performance properties, particularly with respect to heat transfer. Nanofluids are used for cooling of microchips in computers and other electronics which use microfluidic applications. Using nanofluids as coolants would allow for the radiators with smaller sizes and better positioning. An innovative technique, which uses a mixture of nanoparticles and the base fluid, was first introduced by Choi [1] in order to develop advanced heat transfer fluids with substantially higher conductivities. Later, Das et al. [2] experimentally showed a two - to four - fold increase in thermal conductivity enhancement for water-based nanofluids containing Al_2O_3 or CuO nanoparticles over a small temperature range, $21^\circ - 51^\circ C$. A comprehensive survey of convective transport in nanofluids has been made by Buongiorno[3], who gave a satisfactory explanation for the abnormal increase of the thermal conductivity. Buongiorno and Hu [4], studied on the nanofluid coolants in advanced nuclear systems. Ahmad and Pop [5] investigated mixed convection boundary layer flow from a vertical flat plate embedded in a porous medium filled with nanofluids. Boundary layer flow of nanofluids over a moving surface in a flowing fluid was examined by Bachok et al. [6]. Khan and Pop [7] discussed the boundary-layer flow of a nanofluid past a stretching sheet. Makinde and Aziz [8] explained the boundary layer flow of a nanofluid past a stretching sheet with a convective boundary condition. Daungthongsuk and Wongwises [9] studied analytically the effect of thermophysical properties models, for predicting the convective heat transfer rate for low concentration nanofluid.

The study of MHD boundary layer flow on a continuous stretching sheet has attracted considerable attention during the last few decades due to its numerous applications in industrial manufacturing processes. In particular, the

metallurgical processes such as drawing, annealing and tinning of copper wires involve cooling of continuous strips or filaments by drawing them through a quiescent fluid. Controlling the rate of cooling in these processes can affect the properties of the final product. This can be done by using an electrically-conducting fluid and applying a magnetic field. Chamkha and Aly [10] analyzed MHD free convective flow of a nanofluid past a vertical plate in the presence of heat generation / absorption. Rosmila *et al.* [11] discussed MHD natural convection flow of a nanofluid over a linearly porous stretching sheet in the presence of thermal stratification using Lie symmetry group transformation. Ferdows *et al.* [12] studied a mixed convective MHD boundary layer flow of a nanofluid through a porous medium due to an exponentially stretching sheet. Khan *et al.* [13] discussed in detail the MHD boundary layer slip flow of a nanofluid over a convectively heated stretching sheet with heat generation. Sarma *et al.* [14] analyzed a study of MHD free convection heat and mass transfer from vertical surfaces in porous media considering Soret and Dufour effects. Sarkar *et al.* [15] considered the effects of radiation on transient MHD free convective Couette flow in a rotating system. Jayabharath Reddy *et al.* [16] analyzed the mass transfer effects on MHD unsteady free convective flow with constant suction and heat sink through porous media. Vidyasagar *et al.* [17] studied the mass transfer effects on radiative MHD flow over a non isothermal stretching sheet in a porous medium. Chand *et al.* [18] presented the hall effect on radiating and chemically reacting MHD oscillatory flow in a rotating porous vertical channel in slip flow regime.

At high operating temperatures especially in the field of space technology, radiation effect is quite significant. Many processes in engineering areas occur at high temperatures and the knowledge of radiative heat transfer becomes very important, particularly in designing pertinent equipment. Hady *et al.* [19] investigated the effects of thermal radiation on the viscous flow of a nanofluid and heat transfer over a non-linearly stretching sheet. Olanrewaju & Olanrewaju *et al.* [20] studied the boundary layer flow of nanofluids over a moving surface with radiation effects. Hamid *et al.* [21] analyzed the radiation effects on Marangoni boundary layer flow past a flat plate in a nanofluid. El-Aziz [22] studied the radiation effect on the flow and heat transfer over an unsteady stretching surface. Singh *et al.* [23] investigated the thermal radiation and magnetic field effects on an unsteady stretching permeable sheet in the presence of free stream velocity. Gbadeyan *et al.* [24] studied the boundary layer flow of a nanofluid past a stretching sheet with a convective boundary condition in the presence of magnetic field and thermal radiation. Ibrahim [25] investigated the radiation effects on MHD free convection flow along a stretching surface with viscous dissipation and heat generation. Manna *et al.* [26] studied the effects of radiation on unsteady MHD free convective flow past an oscillating vertical porous plate. Anand Rao *et al.* [27] investigated the radiation effect on an unsteady MHD free convective flow past a vertical porous plate.

Very recently, Kuznetsov and Nield [28] have examined the influence of nanoparticles on the natural convection boundary layer flow past a vertical plate incorporating Brownian motion and thermophoresis treating both the temperature and the nanoparticle fraction as constant along the wall. Further, Nield and Kuznetsov [29] have studied the problem proposed by Cheng and Minkowycz [30] about the natural convection past a vertical plate in a porous medium saturated by a nanofluid taking into account the Brownian motion and thermophoresis. Ali Pakravan and Yaghoubi [31] studied the combined thermophoresis, Brownian motion and Dufour effects on natural convection of nanofluids. All these researchers studied the linear stretching sheet in the nanofluid, but a numerical investigation was done by Rana and Bhargava [32] who studied the steady laminar boundary fluid flow of nanofluid past a non-linear stretching flat surface incorporating the effects of Brownian motion and thermophoresis. Also, more recently, Nadeem and Lee [33] investigated analytically the problem of steady boundary layer flow of nanofluid over an exponential stretching surface including the effects of Brownian motion parameter and thermophoresis parameter.

However, to the best of authors' knowledge, so far no attempt has been made to analyze the simultaneous effects of thermal radiation and magnetic on heat and mass transfer flow of nanofluids over a non-linear stretching sheet. Hence, this problem is investigated. The governing boundary layer equations are reduced to a system of ordinary differential equations using similarity transformations and the resulting equations are then solved numerically using Runge - Kutta fourth order method along with shooting technique. A parametric study is conducted to illustrate the influence of various governing parameters on the velocity, temperature, concentration, skin-friction coefficient, Nusselt number and Sherwood number and discussed in detail.

MATHEMATICAL ANALYSIS

A steady two-dimensional boundary layer flow of an incompressible electrically conducting and radiating nanofluid past a stretching surface is considered under the assumptions that the external pressure on the stretching sheet in the x -direction is having diluted nanoparticles. The x -axis is taken along the stretching surface and y -axis normal to it.

A uniform stress leading to equal and opposite forces is applied along the x - axis so that the sheet is stretched, keeping the origin fixed. The stretching velocity is assumed to be $U_w(x) = U_0 x^m$ where U_0 is the uniform velocity and m ($m \geq 0$) is a constant parameter. The fluid is considered to be a gray, absorbing emitting radiation but non-scattering medium. A uniform magnetic field is applied in the transverse direction to the flow. The fluid is assumed to be slightly conducting, so that the magnetic Reynolds number is much less than unity and hence the induced magnetic field is negligible in comparison with the applied magnetic field. Employing the Oberbeck-Boussinesq approximation, the governing equations of the flow field can be written in the dimensional form as

$$\frac{\partial u}{\partial x} + \frac{\partial v}{\partial y} = 0 \quad (1)$$

$$\frac{\partial p}{\partial x} = \mu \frac{\partial^2 u}{\partial y^2} - \rho_f \left(u \frac{\partial u}{\partial x} + v \frac{\partial u}{\partial y} \right) + \left[(1 - C_\infty) \rho_{f_\infty} \beta_T (T - T_\infty) - (\rho_p - \rho_{f_\infty}) \beta_C (C - C_\infty) \right] g - \sigma B_0^2 u \quad (2)$$

$$u \frac{\partial T}{\partial x} + v \frac{\partial T}{\partial y} = \alpha \nabla^2 T + \tau \left\{ D_B \left(\frac{\partial T}{\partial y} \frac{\partial C}{\partial y} \right) + \frac{D_T}{T_\infty} \left(\frac{\partial T}{\partial x} \right)^2 \right\} - \frac{1}{(\rho C)_f} \frac{\partial q_r}{\partial y} \quad (3)$$

$$u \frac{\partial C}{\partial x} + v \frac{\partial C}{\partial y} = D_B \frac{\partial^2 C}{\partial y^2} + \frac{D_T}{T_\infty} \frac{\partial^2 T}{\partial y^2} \quad (4)$$

where u and v are the velocity components in the x and y - directions, respectively, g is the acceleration due to gravity, μ - the viscosity, ρ_f - the density of the base fluid, ρ_p - the density of the nanoparticle, β_T - the coefficient of volumetric thermal expansion, β_C - the coefficient of volumetric concentration expansion, T - the temperature of the nanofluid, C - the concentration of the nanofluid, T_w and C_w - the temperature and concentration along the stretching sheet, T_∞ and C_∞ - the ambient temperature and concentration, D_B - the Brownian diffusion coefficient, D_T - the thermophoresis coefficient, B_0 - the magnetic induction, q_r - radiative heat flux, k - the thermal conductivity, $(\rho C)_p$ - the heat capacitance of the nanoparticles, $(\rho C)_f$ - the heat capacitance of the base fluid, $\alpha = k / (\rho c)_f$ is the thermal diffusivity parameter and $\tau = (\rho C)_p / (\rho C)_f$ is the ratio between the effective heat capacity of the nanoparticles material and heat capacity of the fluid.

The associated boundary conditions are

$$\begin{aligned} u = U_w(x) = U_0 x^m, v = 0, T = T_w, C = C_w \quad \text{at } y = 0 \\ u \rightarrow 0, v \rightarrow 0, T \rightarrow T_\infty, C \rightarrow C_\infty \quad \text{as } y \rightarrow \infty \end{aligned} \quad (5)$$

By using the Rosseland approximation (Brewster [34]), the radiative heat flux q_r is given by

$$q_r = - \frac{4\sigma_s}{3k_e} \frac{\partial T^4}{\partial y} \quad (6)$$

where σ_s is the Stephen Boltzmann constant and k_e is the mean absorption coefficient.

It should be noted that by using the Rosseland approximation, the present analysis is limited to optically thick fluids. If the temperature differences within the flow are sufficiently small, then equation (6) can be linearized by expanding T^4 into the Taylor series about T_∞ , which after neglecting higher order terms takes the form

$$T^4 \cong 4T_\infty^3 T - 3T_\infty^4 \quad (7)$$

Then the radiation term in equation (3) takes the form

$$\frac{\partial q_r}{\partial y} = \frac{16\sigma_s T_\infty^3}{3k_e} \frac{\partial^2 T}{\partial y^2} \quad (8)$$

Invoking equation (8), equation (3) gets modified as

$$u \frac{\partial T}{\partial x} + v \frac{\partial T}{\partial y} = \frac{k}{(\rho C_p)_f} \frac{\partial^2 T}{\partial y^2} + \tau \left\{ D_B \left(\frac{\partial T}{\partial y} \frac{\partial C}{\partial y} \right) + \frac{D_T}{T_\infty} \left(\frac{\partial T}{\partial x} \right)^2 \right\} + \frac{16\sigma_s}{3k_e} \frac{T_\infty^3}{(\rho C_p)_f} \frac{\partial^2 T}{\partial y^2} \quad (9)$$

Using the stream function $\psi = \psi(x, y)$, the velocity components u and v are defined as

$$u = \frac{\partial \psi}{\partial y} \text{ and } v = -\frac{\partial \psi}{\partial x}$$

Assuming that the external pressure on the plate, in the direction having diluted nanoparticles, to be constant, the similarity transformations are taken as

$$\begin{aligned} \psi &= \sqrt{\frac{2\nu U_0 x^{m+1}}{m+1}} f(\eta), \quad \theta(\eta) = \frac{T - T_\infty}{T_w - T_\infty}, \quad \phi(\eta) = \frac{C - C_\infty}{C_w - C_\infty}, \quad \eta = y \sqrt{\frac{(m+1)U_0 x^{m-1}}{2\nu}} \\ Nr &= \frac{k_e k}{4\sigma_s T_\infty^3}, \quad R = \frac{4}{3Nr}, \quad \lambda = \frac{Gr}{Re_x^{\frac{3}{2}}}, \quad \delta = \frac{Gm}{Re_x^{\frac{3}{2}}}, \quad Pr = \frac{\nu}{\alpha}, \quad Le = \frac{\nu}{D_B}, \quad \nu = \frac{\mu}{\rho_f} \\ Nb &= \frac{\tau D_B}{\nu} (C_w - C_\infty), \quad Nb = \frac{\tau D_T}{\nu T_\infty} (T_w - T_\infty), \quad Re_x = \frac{u_w(x)x}{\nu}, \\ Gr &= \frac{(1 - C_\infty) \left(\frac{\rho_{f_\infty}}{\rho_f} \right) gn(T_w - T_\infty)}{\nu^2 Re_x^{\frac{1}{2}}}, \quad Gm = \frac{\left(\frac{\rho_P - \rho_{f_\infty}}{\rho_f} \right) gn_1 (C_w - C_\infty)}{\nu^2 Re_x^{\frac{1}{2}}} \end{aligned} \quad (10)$$

In view of the above similarity transformations, the equations (2) - (4) reduce to

$$f''' + ff'' - \frac{2m}{m+1} f'^2 + \frac{2}{m+1} (\lambda\theta - \delta\phi) - Mf' = 0 \quad (11)$$

$$\frac{1}{Pr} (1 + R)\theta'' + f\theta' + Nb\theta'\phi' + Nt\theta'^2 = 0 \quad (12)$$

$$\phi'' + Lef\phi' + \frac{Nt}{Nb}\theta'' = 0 \quad (13)$$

where λ - the buoyancy parameter, δ - the solutal buoyancy parameter, Pr - the Prandtl number, Le - the Lewis number, ν - the kinematic viscosity of the fluid, Nb - the Brownian motion parameter, Nt - the thermophoresis parameter, Re_x - the local Reynolds number based on the stretching velocity, Gr - the local thermal Grashof number, Gm - the local concentration Grashof number and f, θ, ϕ are the dimensionless stream functions, temperature, rescaled nanoparticle volume fraction respectively. Here, β_T and β_C are proportional to x^{-3} , that is $\beta_T = n x^{-3}$ and $\beta_C = n_1 x^{-3}$, where n and n_1 are the constants of proportionality (Makinde and Olanrewaju, [35]).

The corresponding boundary conditions are

$$\begin{aligned} f = 0, \quad f' = 1, \quad \theta = 1, \quad \phi = 1 \quad \text{at } \eta = 0 \\ f' \rightarrow 0, \quad \theta \rightarrow 0, \quad \phi \rightarrow 0 \quad \text{as } \eta \rightarrow \infty \end{aligned} \quad (14)$$

For the type of boundary layer flow under consideration, the skin-friction coefficient, Nusselt number and Sherwood number are important physical parameters. Knowing the velocity field, the shearing stress at the plate can be obtained, which in the non-dimensional form (skin-friction coefficient) is given by

$$C_f = \frac{2\tau_w}{\rho U^2} = \frac{2\mu}{\rho U_0^2} \left(\frac{\partial u}{\partial y} \right)_{y=0} = \frac{1}{\sqrt{2(m+1)}} \text{Re}_x^{1/2} f''(0) \quad (15)$$

Knowing the temperature field, the heat transfer coefficient at the plate can be obtained, which in the non-dimensional form, in terms of the Nusselt number, is given by

$$Nu = \frac{q_w x}{k(T_w - T_\infty)} = - \frac{q_w}{(T_w - T_\infty)} \left(\frac{\partial T}{\partial y} \right)_{y=0} = - \sqrt{\frac{2}{m+1}} \text{Re}_x^{-1/2} \theta'(0) \quad (16)$$

Knowing the concentration field, the mass transfer coefficient at the plate can be obtained, which in the non-dimensional form, in terms of the Sherwood number, is given by

$$Sh = \frac{q_m x}{k(C_w - C_\infty)} = - \frac{q_m}{(C_w - C_\infty)} \left(\frac{\partial C}{\partial y} \right)_{y=0} = - \sqrt{\frac{2}{m+1}} \text{Re}_x^{-1/2} \phi'(0) \quad (17)$$

SOLUTION OF THE PROBLEM

The set of coupled non-linear boundary layer equations (11) – (13) together with the boundary conditions (14) does not possess a closed form analytical solution. Hence, it has been solved numerically, using the Runge-Kutta method with a systematic guessing of $f''(0)$, $\theta'(0)$, and $\phi'(0)$ by the shooting technique until the boundary conditions at infinity $f''(\infty)$, $\theta'(\infty)$, and $\phi'(\infty)$ decay exponentially to zero. The value of η_∞ is found to each iteration loop by the assignment statement $\eta_\infty = \eta_\infty + \Delta\eta$. The maximum value of η_∞ , to each group of parameters N , n , Nr , Nb , and Nt , is determined when the values of unknown boundary conditions at $\eta = 0$ do not change to a successful loop with error less than 10^{-7} . The step size $\Delta\eta = 0.05$ is used while obtaining the numerical solution with $\eta_{\max} = 10$ and by considering the six decimal place as the criterion for convergence. From the process of numerical computation, the skin-friction coefficient, Nusselt number and Sherwood number, which are respectively proportional to $f''(0)$, $-\theta'(0)$ and $-\phi'(0)$ are also sorted out and their numerical values are presented in tabular form.

RESULTS AND DISCUSSION

In order to get a physical insight into the problem, a parametric study is conducted to illustrate the effects of different governing parameters viz., the magnetic parameter (M), the thermal buoyancy parameter (λ), the solutal buoyancy parameter (δ), the radiation parameter (R), the Prandtl number (Pr), the Schmidt number (Sc), the Lewis number (Le), the thermophoretic parameter (Nt) and the Brownian motion parameter (Nb) upon the nature of flow and transport and the numerical results are depicted graphically in Figs.1 - 21. Here the value of Pr is chosen as 0.71, which corresponds to air. The values of Sc are chosen such that they represent Helium (0.3), water vapor (0.62) and Ammonia (0.78). The other parameters are chosen arbitrarily. The present results are compared with that of Anwar et al. [36] and Khan and Pop [37] (reduced cases) and found that there is an excellent agreement (Table 2).

Fig.1 shows the effect of the Prandtl number on the velocity. It is observed that, an increase in the Prandtl number makes the fluid to be more viscous, which leads to a decrease in the velocity. Fig.2 depicts the effect of thermal buoyancy parameter on the velocity. Here, the positive buoyancy force acts like a favorable pressure gradient and

hence accelerates the fluid in the boundary layer. This results in higher velocity as λ increases. The effect of the solutal buoyancy parameter on the velocity is illustrated in Fig. 3. It is seen that as the solutal buoyancy parameter increases, the velocity decreases. The effect of the stretching parameter on the velocity is presented in Fig.4. It is noticed that, the velocity decreases as the stretching parameter increases. The influence of the magnetic parameter on the velocity is shown in Fig.5. As the magnetic parameter increases, the velocity decreases. This is because, an application of the magnetic field within the boundary layer produces a resistive - type force known as Lorentz force which opposes the flow, and decelerates the fluid motion. Fig. 6 shows the effect of the radiation parameter on the velocity. It is seen that as the radiation parameter increases, the velocity increases.

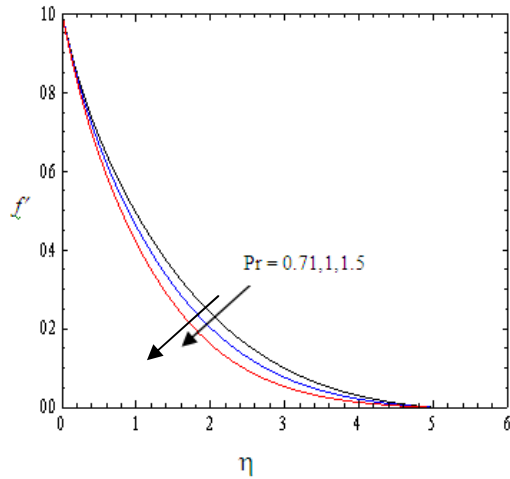


Fig.1. Effect of Pr on Velocity

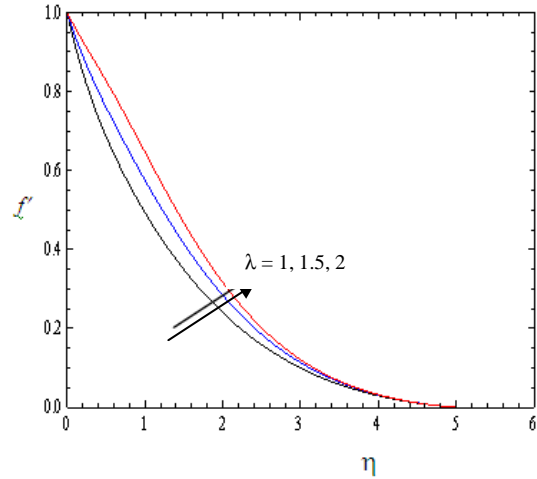


Fig.2. Velocity profiles for different values of λ

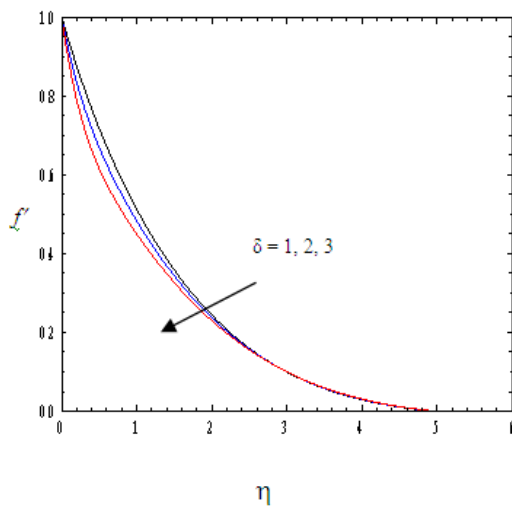


Fig.3. Velocity profiles for different values of δ

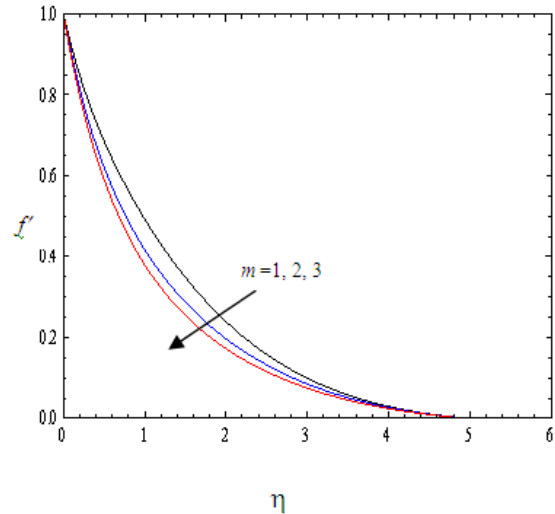


Fig.4. Velocity profiles for different values of m

Fig.7 shows the effect of the Prandtl number on the temperature. It is observed that as the Prandtl number increases, the temperature decreases. This is due to the fact that for smaller values of Pr are equivalent to larger values of thermal conductivities and therefore heat is able to diffuse away from the stretching sheet. The influence of the thermal and solutal buoyancy parameters are illustrated in Figs. 8 and 9. It is clear that the temperature increases, as the thermal or solutal buoyancy parameter increases. The effect of the stretching parameter on the temperature is presented in Fig. 10. It is seen that the temperature increases as the stretching parameter increases. The temperature profiles for different values of the magnetic field parameter are depicted in Fig. 11. It is observed that the temperature increases, as the magnetic field parameter increases. This is due to the fact that the nanoparticles

dissipates energy in the form of heat which causes the thermal boundary layer thickness to increase and ultimately a localized rise in temperature of the fluid occurs. The effect of the radiation parameter on the temperature is depicted in Fig.12. It is seen that as the radiation parameter increases, the temperature increases. The radiation parameter Nr being the reciprocal of the Stark number (also known as Stephan number) is the measure of relative importance of the thermal radiation transfer to the conduction heat transfer. Thus larger values of Nr show a dominance of the thermal radiation over conduction. Consequently larger values of Nr are indicative of larger amount of radiative heat energy being poured into the system, causing a rise in $\theta(\eta)$. The temperature profiles for different values of the Brownian motion parameter and thermophoresis parameter is shown in Figs. 13 and 14, respectively. It is observed that the temperature of the flow field increases as the Brownian motion parameter or thermophoresis parameter increases.

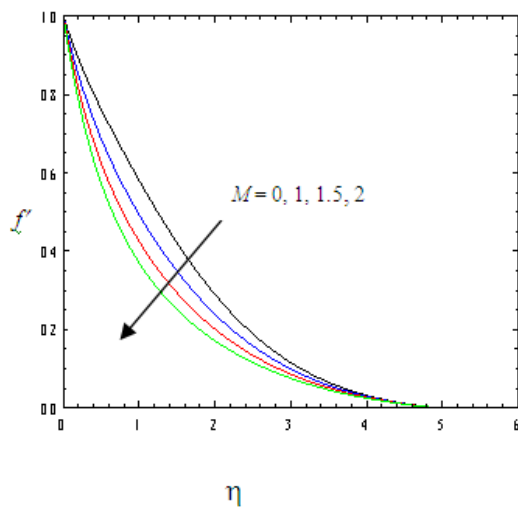


Fig.5. Velocity profiles for different values of M

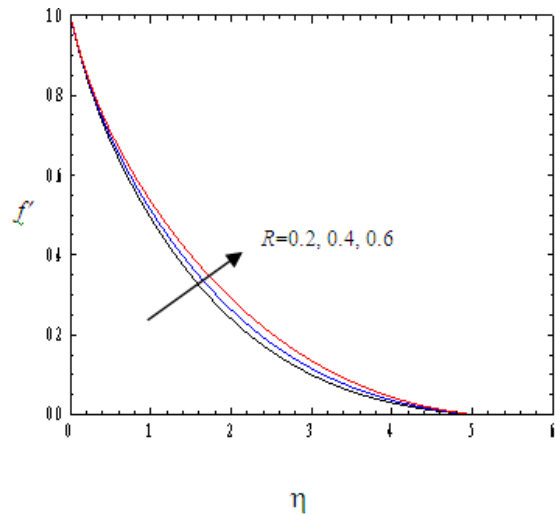


Fig.6. Velocity profiles for different values of R

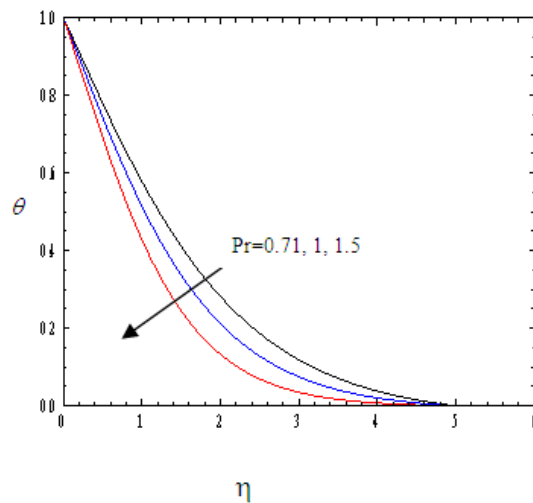


Fig.7. Effect of Pr on the temperature

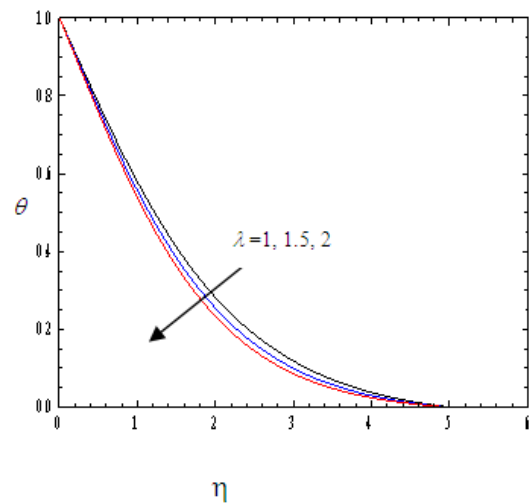


Fig.8. Effect of λ on the temperature

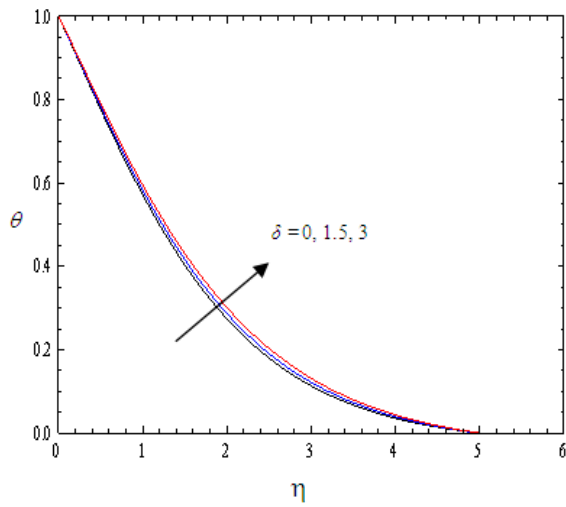


Fig.9. Temperature profiles for different values of δ

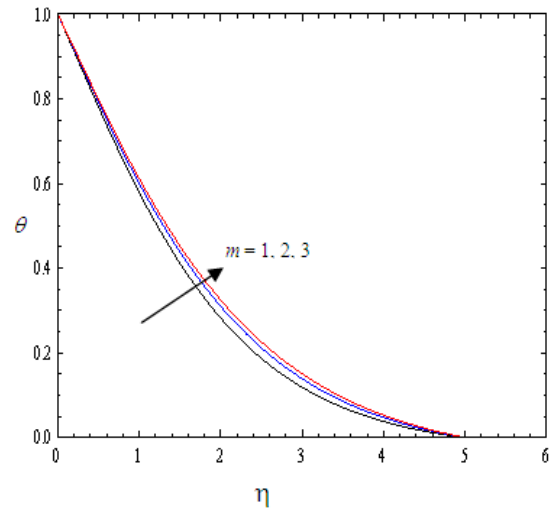


Fig.10. Effect of m on temperature

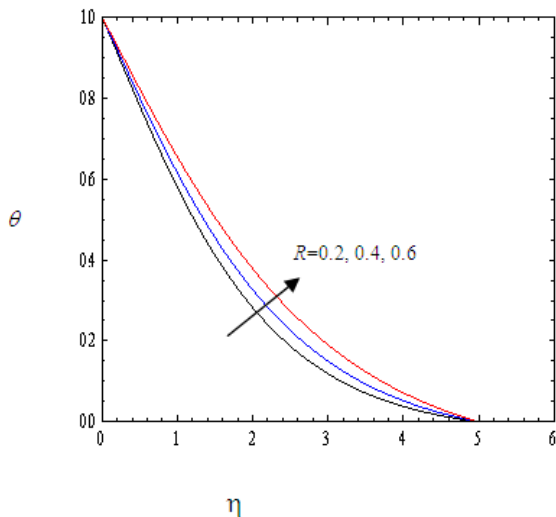


Fig.11. Effect of R on the temperature

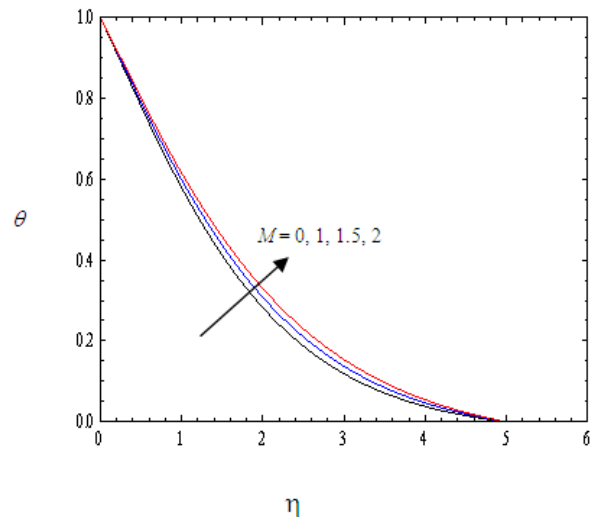


Fig.12. Effect of M on the temperature

Fig.15 shows the effect of the Brownian motion parameter on the concentration. It is noticed that as the Brownian motion parameter increases, the concentration increases. The effect of the thermophoresis parameter on the concentration of the flow field is presented in Fig. 16. We notice that, positive Nt indicates a cold surface while negative to a hot surface. It is seen that the concentration decreases, as the thermophoresis parameter increases. The effect of the magnetic parameter on the concentration field is shown in Fig .17. It is shown that an increase in the magnetic parameter causes an increase in the concentration. Fig. 18 illustrates the effect of the Lewis number on the concentration. It is observed that the concentration decreases as the Lewis number increases. This is due to the fact that there is a decrease in the nanoparticle volume fraction boundary layer thickness with the increase in the Lewis number. The influences of the thermal and solutal buoyancy parameters on the concentration field are shown in Fig.19 and 20, respectively. It is noticed that the concentration decreases as the thermal or solutal buoyancy parameter increases. Fig. 21 shows the effect of the radiation parameter on the concentration. It is noticed that the concentration decreases as the radiation parameter increases.

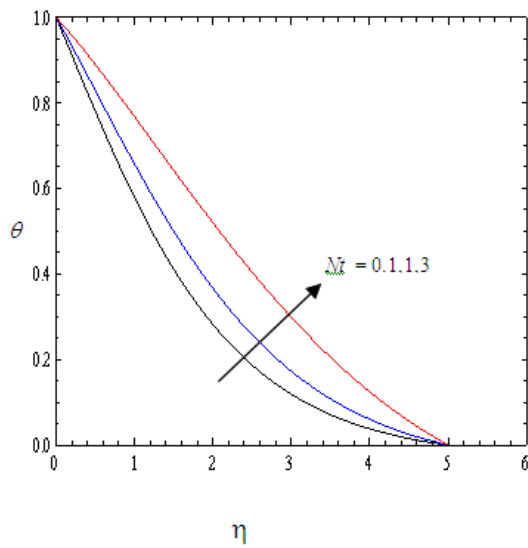


Fig.13. Effect of Nt on temperature

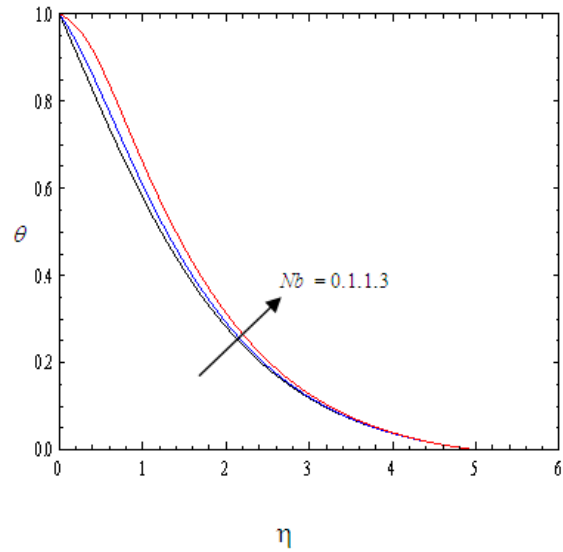


Fig.14. Effect of Nb on temperature

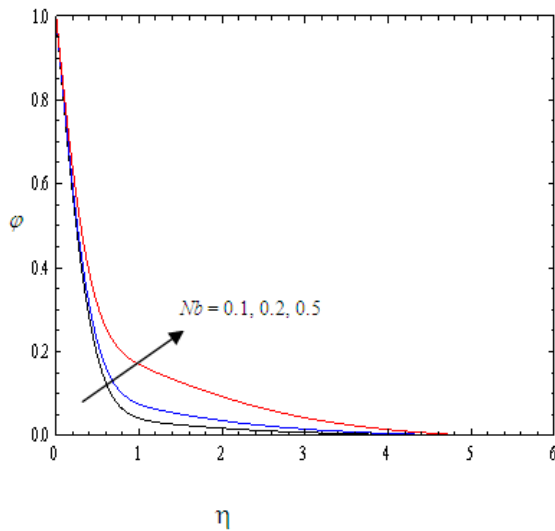


Fig.15. Concentration profiles for distinct values of Nb

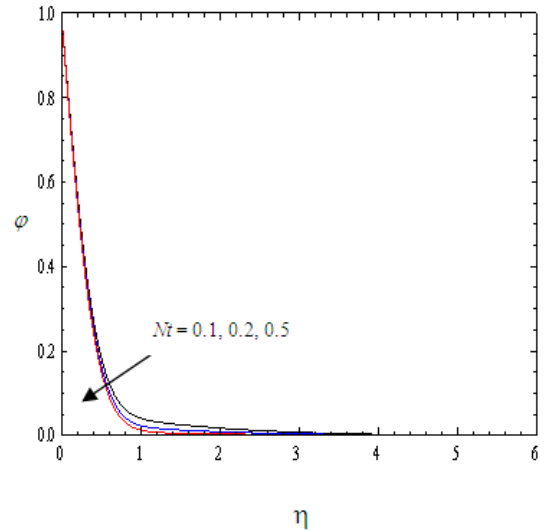


Fig.16. Concentration profiles for different values of Nt

Table 1 shows the computations of the skin-friction coefficient, Nusselt number and the Sherwood number for various physical parameters. It is observed that as M increases, both the skin-friction coefficient and Nusselt number increase whereas the Sherwood number decreases. An increase in the radiation parameter leads to a rise in the Nusselt number and Sherwood number and a fall in the skin-friction coefficient. As λ increases, both the skin-friction coefficient and Sherwood number decrease while the Nusselt number increases. It is observed that an increase in δ , leads to an increase in the skin-friction coefficient and a decrease in the Nusselt number and Sherwood number. An increase in Le shows a decreasing trend in the skin-friction coefficient and Nusselt number while an increasing trend in the Sherwood number. As Nt increases, both the skin friction coefficient and Nusselt number increase rapidly whereas the Sherwood number decreases. With an increase in the values of Nb , both the skin friction coefficient and Nusselt number decrease whereas the Sherwood number increases.

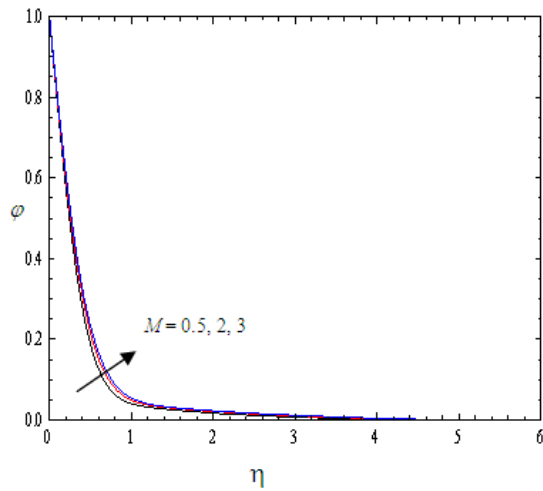


Fig.17. Concentration profiles for different values of M

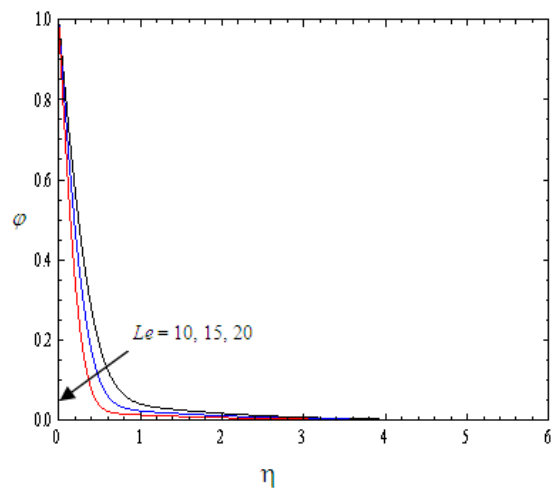


Fig.18. Concentration profiles for distinct values of Le

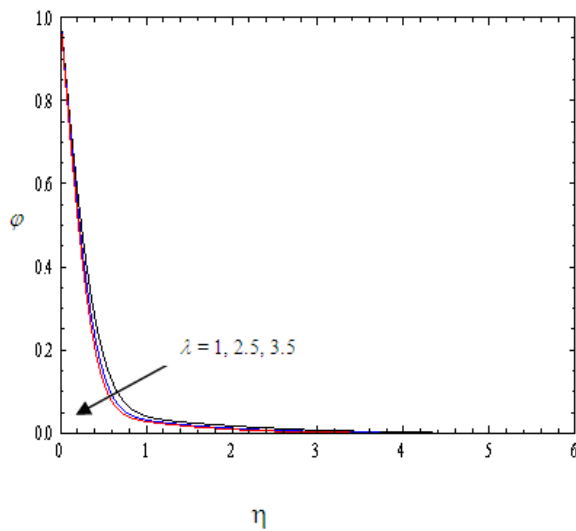


Fig.19. Concentration profiles for different values of λ

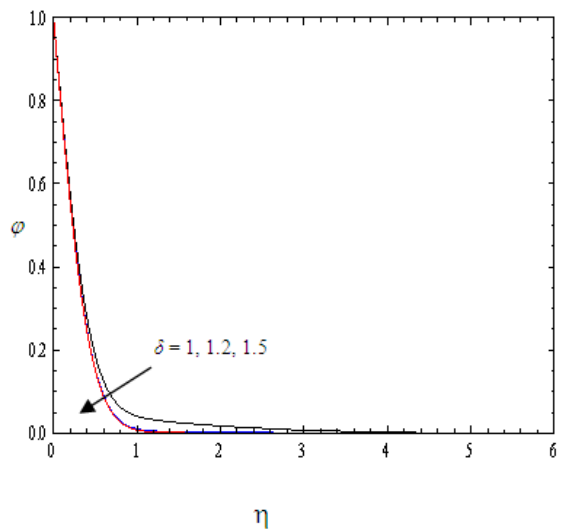


Fig.20. Concentration profiles for different values of δ

Table 1 Computations of the skin friction coefficient, Nusselt number and the Sherwood number for various values of $Nb, Nt, Pr, Le, \lambda, \delta, m$

Nb	Nt	Pr	Le	λ	δ	m	R	M	$-\theta'(0)$	$-\phi'(0)$	$f''(0)$
0.1	0.1	0.71	10	1	1	1	0.2	0.5	0.4281	2.25624	0.8849
0.5	0.1	0.71	10	1	1	1	0.2	0.5	0.3505	2.3507	0.86033
0.1	0.5	0.71	10	1	1	1	0.2	0.5	0.375241	1.9571	0.93743
0.1	0.1	10	10	1	1	1	0.2	0.5	0.9489	2.01739	1.2089
0.1	0.1	0.71	25	1	1	1	0.2	0.5	0.4313	3.7695	0.81168
0.1	0.1	0.71	10	2	1	1	0.2	0.5	0.4748	2.3463	0.3962
0.1	0.1	0.71	10	1	2	1	0.2	0.5	0.285103	0.1746	0.88422
0.1	0.1	0.71	10	1	1	3	0.2	0.5	0.3901	2.19	1.18586
0.1	0.1	0.71	10	1	1	1	0.4	0.5	0.3994	2.2722	0.86674
0.1	0.1	0.71	10	1	1	1	0.2	1	0.4050	2.2126	1.10527

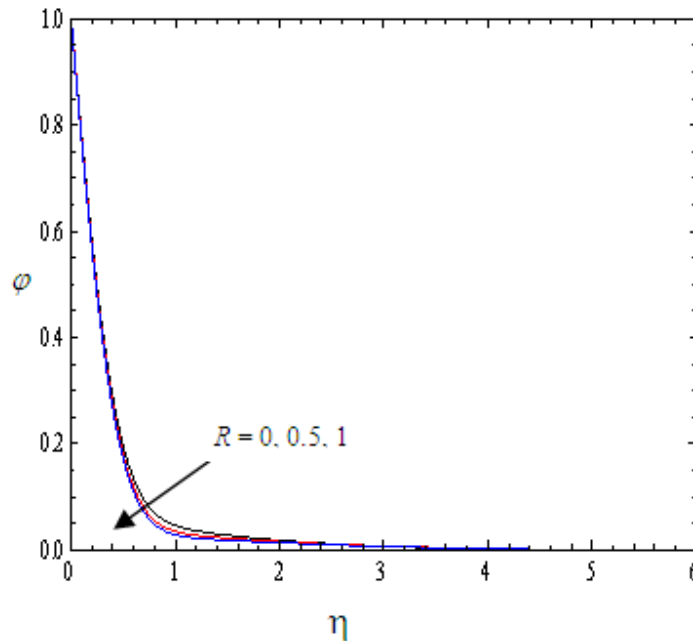


Fig.21. Concentration profiles for different values of R

Table 2 Comparison of reduced Nusselt number, reduced Sherwood number and skin-friction coefficient

Nb	Nt	Pr	Le	λ	δ	m	Khan and Pop (2010)		Anwar and Khan et al. (2012)		Present results	
							$-\theta'(0)$	$-\phi'(0)$	$-\theta'(0)$	$-\phi'(0)$	$-\theta'(0)$	$-\phi'(0)$
0.1	0.1	10	10	0	0	1	0.9524	2.1294	0.9524	2.1294	0.952376	2.12939
0.2	0.2	10	10	0	0	1	0.3654	2.5152	0.3654	2.5152	0.365357	2.51522
0.3	0.3	10	10	0	0	1	0.1355	2.6088	0.1355	2.6088	0.135514	2.60881
0.4	0.4	10	10	0	0	1	0.0495	2.6038	0.0495	2.6038	0.049465	2.60384
0.5	0.5	10	10	0	0	1	0.0179	2.5731	0.0179	2.5731	0.017922	2.5731

CONCLUSION

This study has analyzed the effect of the radiation on a steady MHD heat and mass transfer flow over a non linear stretching sheet. The non-linear governing equations and their associated boundary conditions have been transformed to non dimensional equations using the similarity transformations and the resultant problem is solved by an iterative Runge-Kutta method along with shooting technique. The present results are compared with the existing literature and found a good agreement. The influence of the governing parameters on the velocity, temperature, concentration distribution as well as the skin friction coefficient, heat and mass transfer rates have been systematically examined. From the present numerical investigation, the following inferences can be drawn:

- A rise in the radiation parameter raises the temperature as well as rate of heat transfer and the presence of radiation radiates the heat energy away from the fluid. It is the nanofluids property to enhance the thermal conductivity.
- Velocity accelerates with an increase in the thermal buoyancy force or radiation and decelerates with an increase in the Prandtl number or magnetic field or solutal buoyancy force or stretching parameter.
- There is a rise in the temperature with an increase in the magnetic field or solutal buoyancy force or the radiation or thermophoresis parameter or Brownian motion parameter or stretching parameter and a fall with an increase in the thermal buoyancy parameter or Prandtl number.
- Species concentration increases with an increase in the magnetic field or Brownian motion while the concentration decreases for an increase in the values of the thermophoresis parameter or Lewis number or thermal buoyancy force or solutal buoyancy force or radiation parameter.

- Skin friction coefficient increases with an increase in the magnetic parameter or stretching parameter or solutal buoyancy force or thermophoresis parameter or Brownian motion parameter and decreases with an increase in the radiation parameter or Lewis number.
- Heat transfer rate rises with a rise in the magnetic parameter or radiation parameter or thermophoresis parameter or Brownian motion parameter and it falls with an increase in the solutal buoyancy parameter or Lewis number.
- Mass transfer rate increases with an increase in the radiation parameter or stretching parameter or Lewis number or Brownian motion parameter and decreases with an increase in the magnetic parameter or solutal buoyancy parameter or thermophoresis parameter.

REFERENCES

- [1] Choi S: *American Society of Mechanical Engineers*, **1995**, 99–105, New York.
- [2] Das S K, Putra N, Thiesen P, and Roetzel W: *J. Heat Transfer*, **2003**, 125, pp.567–574.
- [3] Buongiorno J: *ASME J. Heat Transfer*, **2006**, 128, 240–250.
- [4] Buongiorno J, Hu : Nanofluid coolants for advanced nuclear power plants. Paper no. 5705, *Proceedings of ICAPP '05*, Seoul, May 15–19, **2005**.
- [5] Ahmad S and Pop I, *International Communications in Heat and Mass Transfer*, **2010**, 37, pp.987-991.
- [6] Bachok N, Ishak A, Pop I, *International Journal of Thermal Sciences*, **2010**, 49, 1663-1668.
- [7] Khan W A and Pop I, *International Journal of Heat and Mass Transfer*, **2010**, vol. 53, no. 11-12, pp. 2477–2483.
- [8] Makinde O D and Aziz A, *International Journal of Thermal Sciences*, **2011**, Vol. 50, Issue 7, July 2011, pp. 1326–1332.
- [9] Daungthongsuk W and Wongwiset S, *International Communications in Heat and Mass Transfer*, **2008**, 35, pp.1320-1326.
- [10] Chamkha A J & Aly A M, *Chem. Eng. Comm.*, **2011**, 198, pp.425–441.
- [11] Rosmila A B, Kandasamy R, Muhaimin I, *Appl. Math. Mech. -Engl. Ed.*, **2012**, 33(5), 593–604.
- [12] Ferdows Md. M, Shakhaoath Khan Md., Mahmud Alam and Shuyu Sun, *Mathematical Problems in Engineering*, Volume **2012**.
- [13] Md. Jashim Uddin, Khan W A, and Md. Ismail A I, *Mathematical Problems in Engineering*, **2012**.
- [14] G. Sreedhar Sarma, Sreenivasu D, Govardhan K, Ramakrishna Prasad K, , *Advances in Applied Science Research*, Pelagia Research Library, **2013**, 4(1):300-307.
- [15] Bhaskar Chandra Sarkar, Sanatan Das and Rabindra Nath Jana, *Advances in Applied Science Research*, Pelagia Research Library, **2012**, 3 (5):3291-3310.
- [16] Jayabharath Reddy M, Jayarami Reddy and Sivaiah G, *Advances in Applied Science Research*, Pelagia Research Library, **2012**, 3 (2):1137-1143.
- [17] Vidyasagar G, Bala Anki Reddy P, Ramana B and Sugunamma V, *Advances in Applied Science Research*, Pelagia Research Library, **2012**, 3 (6):4016-4029.
- [18] Chand K, Singh K D and Kumar S, *Advances in Applied Science Research*, Pelagia Research Library **2012**, 3 (4):2424-2437.
- [19] Fekry M Hady, Fouad S Ibrahim, Sahar M Abdel-Gaied and Mohamed R Eid, *Nanoscale Research Letters*, **2012**.
- [20] Olanrewaju, P O, Olanrewaju, M A and Adesanya A O, *International Journal of Applied Science and Technology*, Vol. 2 No. 1; January **2012**.
- [21] Rohana Abdul Hamid, Norihan Md. Arifin, Roslinda Mohd Nazar, and Ioan Pop, Radiation effects on Marangoni boundary layer flow past a flat plate in nanofluid. *Proceedings of the International Multiconference of Engineers and Computer Scientists*, **2011**, Vol II , Hongkong.
- [22] El-Aziz M A, *Int. Commu. Heat and Mass Transf.*, **2009**, 36, 521–524.
- [23] Singh P, Jangid A, Tomer NS, Sinha D, *Int. J. Info. and Math. Sci*, 6, 3, **2010**.
- [24] Gbadeyan JA, Olanrewaju M A, and Olanrewaju, *Australian Journal of Basic and Applied Sciences*, **2011**, 5(9): 1323-1334.
- [25] S Mohammed Ibrahim, *Advances in Applied Science Research*, Pelagia Research Library, **2013**, 4(1), pp.371-382.
- [26] Sib Sankar Manna, Sanatan Das and Rabindra Nath Jana, *Advances in Applied Science Research*, Pelagia Research Library, **2012**, 3 (6):3722-3736.
- [27] Anand Rao, Shivaiah S and Nuslin Sk, *Advances in Applied Science Research*, Pelagia Research Library, **2012**, 3 (3):1663-1676
- [28] Kuznetsov VA and Nield D A , *International Journal of Thermal Sciences*, **2010**, vol. 49, no. 2, pp. 243–247.

- [29] Nield DA and Kuznetsov A V , *International Journal of Heat and Mass Transfer*, **2009**,vol.52, no. 25-26, pp. 5792–5795.
- [30] Cheng P and Minkowycz W J, *Journal of Geophysical Research*, **1977**, 82, 2040-2044.
- [31] Hossein Ali Pakravan, Mahmood Yaghoubi, *International Journal of Thermal Sciences xxx* ,**2010**, pp.1 - 9.
- [32] Rana P, Bhargava R, *Commun Nonlinear SciNumer Simulat*, **2011**,17(1):212-226.
- [33] Nadeem S, Lee C , *Nanoscale Res Lett* ,**2012**, 7:94.
- [34] Brewster MQ: Boundary layer growth on a flat plate with suction or injection, *J.Phys.Soc.Japan*, **1972**,Vol.12, pp.68-72.
- [35] Makinde OD, Olanrewaju PO, *J. Fluids Eng. Trans. ASME*, **2010**,132:044502-1-4.
- [36] Anwar M I, Khan I, Sharidan S. and Salleh M Z, *International Journal of Physical Sciences*,**2012** Vol. 7(26), pp. 4081 - 4092.
- [37] Khan WA, Pop I, *Int J Heat Mass Transf.* **2010**, 53:2477-2483.